

# On Linearisation of Microwave-Transmitter Solid-State Power Amplifiers

M. O'Droma,<sup>1</sup> E. Bertran,<sup>3</sup> J. Portilla,<sup>2</sup> N. Mgebrishvili,<sup>1</sup> S. Donati Guerrieri,<sup>4</sup>  
G. Montoro,<sup>3</sup> T. J. Brazil,<sup>5</sup> G. Magerl<sup>6</sup>

<sup>1</sup> University of Limerick, Ireland

<sup>2</sup> University of the Basque Country (UPV-EHU), Bilbao, Spain

<sup>3</sup> UPC, Barcelona, Spain

<sup>4</sup> Politecnico Di Torino, Italy

<sup>5</sup> National University of Ireland, Dublin

<sup>6</sup> Technical University of Vienna, Austria

Received 22 November 2004; accepted 11 May 2005

**ABSTRACT:** Developments in new and classical RF solid-state power amplifier (SSPA) linearisation techniques, within the context of the EU TARGET (“Top Amplifier Research Groups in a European Team”) Network of Excellence’s (NoE’s) coordination of research in this field, are reviewed. The issues addressed include feedforward, digital, and analog predistortion; feedback (at both circuit and system levels); and context-based bounds for linearisation benefits. © 2005 Wiley Periodicals, Inc. *Int J RF and Microwave CAE* 15: 491–505, 2005.

**Keywords:** power amplifier; linearisation; percentage linearisation; predistortion linearisation; feedforward linearisation

## I. INTRODUCTION

Mobile wireless networks are evolving towards wider bandwidths and higher spectral efficiency (bits/Hz), and are using multilevel nonconstant envelope modulation (NoCEM) schemes (for example, M-QAM), at higher air-interface frequencies. Handsets, base stations, high-altitude platforms (HAPs), LMDS, and satellites—all types of access nodes—are already being required to handle air-interface modes with high-signal-envelope crest factors, that is, high peak-to-average-power ratio (PAPR). In bandwidth-efficient, multilevel, NoCEM (for example, M-QAM) wireless systems, the linearity of the transmitter and especially of the RF power amplifier (PA) is of key importance.

Hence, PA linearisation for ameliorating in-band and out-of-band nonlinear PA impairment effects in a cost-efficient way is currently a very active research topic.

The theory, principles, and techniques of PA linearisation have been evolving since the early days of wireless transmitters. Techniques include analog and digital predistortion, feed-forward, direct and indirect RF feedback techniques, EER, polar loop, Cartesian loop, LINC, and other cancellation methods. An abbreviated historical approximate assessment of some core attributes of many of these is given in Table I. Other attributes of systems and circuits that also need to be considered now include dynamic/static, adaptive/nonadaptive, baseband/IF/RF, and memoryless/memory-effects tracking and compensation. Implementation considerations include a scheme’s complexity, stability, robustness, reliability, energy efficiency, size, weight, thermal considerations, and cost. Implementation may be at the circuit or system

Correspondence to: M. O’Droma; e-mail: mairtin.odroma@ul.ie.  
DOI 10.1002/mmce.20114  
Published online 21 July 2005 in Wiley InterScience (www.interscience.wiley.com).

TABLE I. Some Historical Approximate Indicators of Linearity Schemes

Technique	Year	RF BW [MHz]	Linearity Improvement [IM3 dBc]	Power-Efficiency Improvement	Comments
Distortion feedback	1930	<20	2–4	Low	Low bandwidth, instability
Envelope feedback	1960	<20	4–15	Moderate	Detector linearity, low bandwidth
Polar feedback	1970	<20	5–40	Moderate	Detector linearity, delays, PLL instability
Doherty	1936	High	—	None	Not properly a lineariser
Power backoff	—	High	40–70	None	High cost (low efficiency)
LINC/CALLUM	1974/ 1992	<20	40–65	High (+)	PA's equilibrium (LINC) + implementation of $\cos^{-1}$ Instability (CALLUM) + Cost
EER	1952	<15	10–35	High (++)	Delays, time constant, detector linearity
Diode predistortion	1970	<30	3–30 (3–6)	Moderate	Critical adjustments
Adaptive predistortion	1980 (90)	<50	20–50	Low (DSP)	DSP + ADC: Cost LUT adjustment time
Feed-forward	1940 (60)	>100	20–40 (40–60)	Low (2 <sup>nd</sup> amplifier)	Phase delays compensation, Auxiliary amplifier
Cartesian feedback	1980	<20	10–50 [f(BW)]	Alta	Low bandwidth, Instability, I and Q modulation
Data feedback	1990	—	—	Moderate (DSP)	Modulation sensitive, DSP, COST, no ACPR control

level, with the former usually having the attractions of lower energy consumption, simpler design, and being “MMIC-integratable.” Lineariser and PA analysis and design tools are growing in number and sophistication, and these include device-, circuit-, system-, and behavioural-level simulation, modelling, and performance-prediction tools.

By addressing linearisation techniques, issues, and challenges, this article provides insight about some specific new and interesting developments in a number of classical linearisation schemes; an introduction to lineariser adaptivity capabilities for responding to transient SSPAs effects (for example, dynamic memory and thermal effects) and transient lineariser-SSPA circuit and system effects; and a brief review of linearity indicators and evaluation criteria. The article especially reflects ongoing linearisation research within the EU TARGET (“Top Amplifier Research Groups in a European Team”) Network of Excellence (NoE) [1].

## II. BACKGROUND POWER-AMPLIFIER ISSUES

Amplifier power-added efficiency (PAE) and linearity are competing requirements. The typical PAE versus

PA backoff curve shows poor PAE performance with PA operation (for most amplifier classes) in the linear region but “takes off” roughly along a raised sine (RS)-shaped curve as it moves into the nonlinear region. Where it peaks in this nonlinear region varies from device to device and, of course, is dependent on the amplifier class. However, the peak value of PAE, and even the significant PAE improvements available, are usually beyond the PA's 1-dB compression point (P1dB) (see, for example, [2–6]). Achieving linear operation by operating point backoff will thus be at the expense of PAE. Hence, inclusion of a lineariser which enables better PAE operation is likely to be attractive. How attractive is, of course, also related to acceptable cost ratios of lineariser performance and manufacturability.

There are significant transient memory and thermal effects being observed in new SSPA device technology, especially in the drive for ever higher frequency and output-power capability. Apart from the problems arising due to incorrectly-tuned bias circuits [7], SSPAs are extremely temperature sensitive, with the impact of self-heating occurrences affecting their RF performance. For example, Capelluti et al. [8] reported on successful circuit-level harmonic-balance frequency-domain simulations of a coupled electrical and thermal model, illustrating the process of the DC

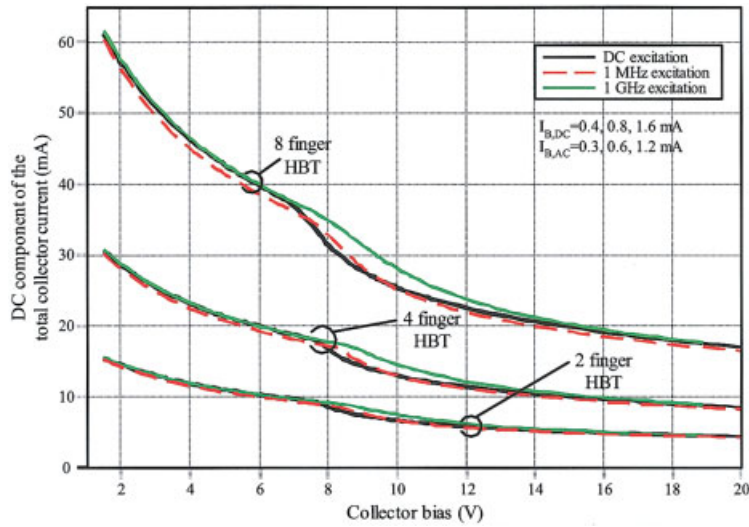


**Figure 1.** Dynamic electrothermal simulation of DC thermal collapse in a power HBT with one input tone at different frequencies. [Color figure can be viewed in the online issue, which is available at [www.interscience.wiley.com](http://www.interscience.wiley.com).]

thermal collapse of a power HBT with one input tone at different frequencies (Fig. 1). Another known phenomenon is the modulation of the operating temperature by the signal envelope of large PAPR drive signals in some instances. In such contexts, the char-

acterization of the SSPA nonlinearity, and thus of the impairments caused by this nonlinearity, becomes a dynamic matter, and the linearisers seeking to offset the nonlinearity effects need to adapt dynamically. As RF operating frequencies increase up to several GHz,

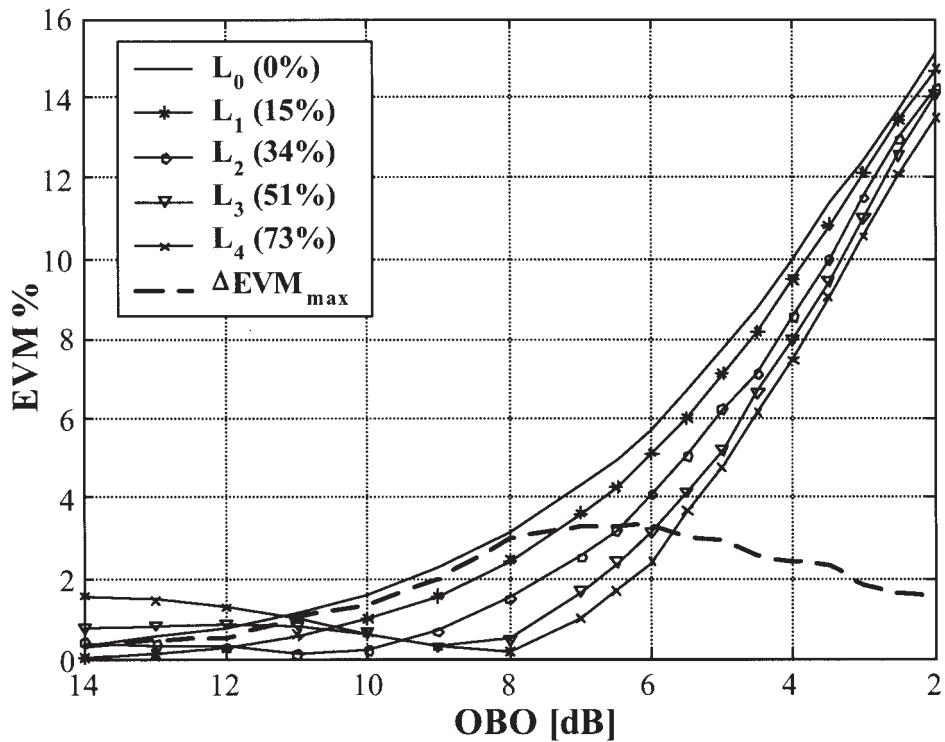


**Figure 2.** Linearisation EVM improvement, and maximum available EVM benefit, for a IEEE 802.11a OFDM signal through a pHEMT SSPA as a function of PL and OBO.

and signal-amplification bandwidths become greater (for example, >50 MHz per single-mode channel, with a growing demand for simultaneous multimode channels) the challenge to find linearisation solutions becomes more urgent. An early step in this work involves research into accurate dynamic modelling and measurement of self-heating so as to better understand and characterise these effects. Research goals of temperature, time, and space resolution for measurements of these effects in the TARGET NoE are 5°K, 2 ns, and 2  $\mu$ m, respectively.

### III. LINEARITY INDICATORS, EVALUATION CRITERIA, AND STANDARDS

Traditional device and circuit PA linearity indicators tend to be focused on measures such as the PA's 1 dB compression point, P1 dB, the two-tone third-order intermodulation product ( $IM_3$ ) intercept point (3IP), and  $IM_3$  suppression graphs, such as the carrier to  $IM_3$  ( $C/I_3$ ) versus PA backoff. However, more sophisticated inputs have been advised [9, 10] in device- and circuit-characterisation measurements in order to yield more accurate total intermodulation distortion (IMD) results. In any case, it is usually considered that only a few dB improvement of IMD can have a significant performance impact.

Behaviourally, at a system level, nonlinearity is gauged by (i) the interference caused in the adjacent channels, typically given as an adjacent-channel-power ratio (ACPR) measure, and (ii) the deterioration in modulation fidelity (MF) of the transmitted signal (or signals in the case of simultaneous multimode), visible in eye and constellation diagrams and usually measured as an error-vector magnitude (EVM) extracted from the latter. ACPR and EVM measures are not independent, as both are caused by the same nonlinearity process [11]. A new relative measure of the degree of linearisation, called percentage linearisation (PL), has been introduced and linked to the behavioural measures such as EVM, ACPR, and  $C/I_3$  [12]. PL has the potential to enable a comparison between different linearisation techniques, thus assessing the potential benefit of introducing a linearisation scheme in a particular application, as well as the setting of design goals for linearised PAs. In this context, the standard static memoryless or quasi-memoryless [7] PA and lineariser-characteristic models have important benchmark roles, as they are effective at setting upper bounds for lineariser benefits (ACPR, EVM, and so forth) as a function of PL, input backoff (IBO), and output backoff (OBO) and PAE. Figure 2 provides insight with regard to this approach by showing the

EVM improvement as a function of PL vs. OBO w.r.t. the 0.1 dB gain point and maximum available EVM benefit for an IEEE 802.11a OFDM system with a typical memoryless pHEMT PA [9].

## IV. TYPES OF LINEARISATION

In general, there is no "best" linearisation technique. Whichever method is used, it needs to be optimised for the particular system being designed, taking into account the required operating frequencies and bandwidths, the modulation method (for example, single or multicarrier), whether or not the systems is simultaneous, multimode and multiband operation, as well as other factors mentioned above. A selection of some of the interesting linearisation-scheme developments presently underway within TARGET, together with some contextual and evaluative comments, is presented as follows.

### A. Feedback

Negative feedback has been widely employed at low frequencies, but can also provide linearisation if applied directly to the amplifier in the form of RF or IF feedback, envelope feedback, or harmonic feedback (for example, [13, 14]). The use of classical negative feedback at high frequencies has been limited by unavoidable parasitic and time-delay effects. These effects can give rise to instability problems and loss of gain. The problems can be circumvented for narrow-bandwidth applications with careful design. For wider-band systems, feasibility, stability, and robustness difficulties slow up (and likely constrain) the evolution of feedback linearisation [13, 14]. Nonetheless, new developments in fast, accurate linear and nonlinear stability-analysis techniques have demonstrated their suitability for the detection and avoidance of undesired instabilities in medium-power PAs and PAs working under different bias, frequency, or power conditions [15]. These techniques can be helpful in optimising the feedback loop, hence avoiding spurious oscillations and opening up new perspectives in the design of feedback-linearisation strategies.

**Circuit Based Passive Feedback.** Preliminary studies on the application of nonlinear stability-analysis techniques for the circuit design of an L-band medium-power bipolar amplifier<sup>1</sup> with passive feedback (Fig. 3) have demonstrated encouraging results [16]. The

<sup>1</sup> Devices were Infineon BJT ref. BFG13A, specially intended for low-distortion power amplification up to 2 GHz. A typical IMD result for this device is 38-dBm IP3 at 900 MHz.

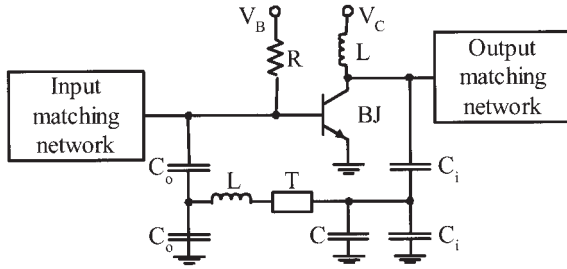


**Figure 3.** L-Band BJT PA with optimised and stable passive feedback.

passive feedback loop is optimised and the stability is checked for different carrier-input power. Improvement of the ACPR, with a QPSK excitation signal, for rates at 10 and 20 MSymbols/sec (though not at 30 MSymbols/sec) is shown in Figure 4. The analysis method used, “transient envelope,” takes into account full nonlinear contributions to the IMD.

**H-infinity Feedback.** H-infinity (H-inf) design-optimization theory applied to feedback linearisers is a new approach that has proven to be effective in improving classical-feedback results. For instance, in conventional classical Cartesian feedback, the closed-loop stability is not assured and stability margins are usually only empirically adjusted. Also, the closed-loop gain (and consequently the PA output power) depends on the feedback. An “H-inf reference feedback” scheme, as shown in Figure 5, was proposed by Bertran et al. [17]. The idea is to feed back the difference (error signal) between an attenuated PA output and a linear reference obtained directly from the source. Two filters, with transfer function  $G_F$ , are included in order to bound the baseband spectral

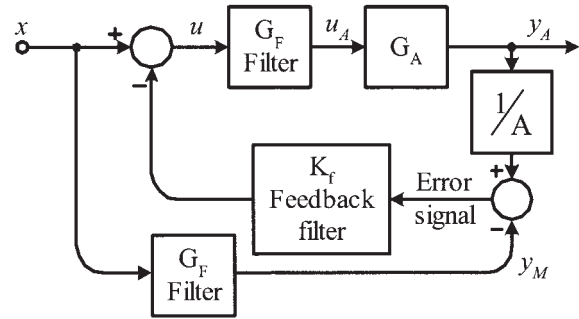


**Figure 5.** H-infinity model reference feedback (H-inf MRF) block diagram.  $G_A$  includes the modulator, amplifier and demodulator; attenuator  $A$  is the desired linear gain;  $\Phi$  is a nonlinear function.

content. The structure has separate feedback paths to process the I and Q baseband signals. With parameters defined as in Figure 5, the overall closed-loop transfer function for the error signal (between  $y_A$  and  $y_M$  signals) for one of the baseband loops (for example, the I component) is given by

$$e = \frac{1}{1 + K_f G_F} \Phi(G_F(u)). \tag{1}$$

The  $K_f$  filter (or gain, in the proportional-feedback case) must minimize the H-inf norm in the transfer function in order to assure closed-loop stability. This depends on the norm of the  $\Phi$  nonlinearity function. The model reference structure, widely used in adaptive control, has the attraction of good closed-loop robustness. With regard to the choice of  $K_f$  and robustness, the results show that output power ( $P_o$ ), PAE, and ACPR are offset smooth near-inverse func-

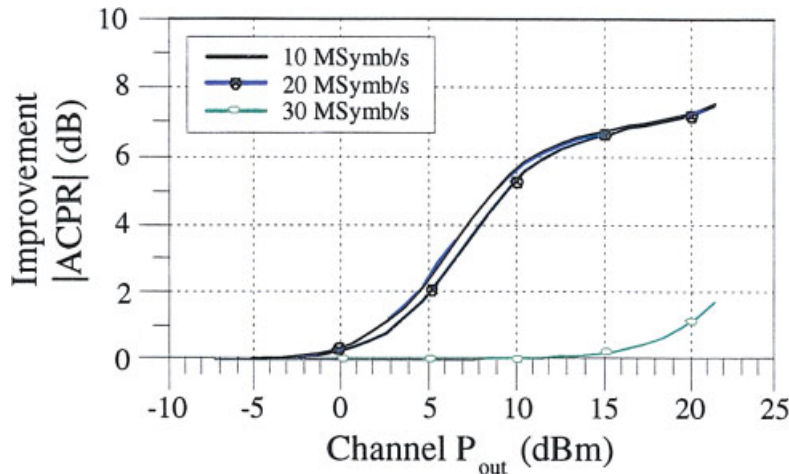


**Figure 4.** ACPR improvement on the passive feedback linearised L-Band PA in Fig. 3 (QPSK excitation).

TABLE II. Comparison of the PA With and Without Cartesian and H-inf Linearisation

	Amplifier	Cartesian Feedback		H-inf Model-Reference Cartesian Feedback
$K$ value	—	$K_2 = 30$ dB	$K_2 = 11$ dB	$K_f = 20$ dB
Output power	20 dBm	16.8 dBm	20.1 dBm	20.2 dBm
Lower ACPR	25.1 dBr	48.8 dBr	34 dBr	77.8 dBr
Upper ACPR	24.5 dBr	47.9 dBr	33.4 dBr	77.5 dBr
PAE	17.3%	6.5%	14.6%	14.7%

tions of  $K_f$  (over the ranges PAE: 13% to 21%;  $P_o$ : 19.6 to 21.6 dBm, ACPR: 164 to  $-80$  dB, and  $K_f$ : 10 to 50). Choosing  $K_f$  to meet the ACPR requirements fixes  $P_o$  and PAE. Table II presents a comparison of the ACPR improvement performance for a PA with and without Cartesian and H-inf linearisation. The superiority of H-inf may be noted. The fact that detailed information about the PA is not required is a further advantage; instead, only a simple bound on the nonlinearities is necessary.

**Hyperstability Feedback.** The hyperstable design of feedback linearisers is another new technique currently attracting attention. These linearisers, which may be implemented in analog circuitry or through DSP, are capable of tolerating significant PA parameter variations, including time variations and device-parameters fluctuation. The design [18] is based on a parallel “model-reference adaptive system” (MRAS), as shown in Figure 6. The reference is formed by a small-signal amplifier (that is, linear), which amplifies voltage only, not current. Hence, its dissipated power, and thus its impact on PAE, is small. Unlike the auxiliary amplifiers used in feedforward structures, the reference amplifier here is not a PA. The adaptive mechanism employs two nonlinear proportional ( $k_2$ ) and integrative ( $k_1$ ) feedback laws: the first to cater for

the dynamics and the second for precision. Hyperstable design has thus a Lur’e form, with linear subsystems in the forward path (a design premise) and nonlinear in the feedback path. The latter need only be “passive” in the system sense in order to assure asymptotic stability. The feedback is incorporated through an analog four-quadrant multiplier,  $w(e, t)$ . For both AM-AM and AM-PM distortion compensation, two feedback paths are required with I and Q quadrature decomposition. The design objective is to drive the error,  $e(t)$ , between the reference model and the actual nonlinear PA to zero (asymptotically), at which point the nonlinear PA will show the same dynamics as the reference linear-amplifier model.

The C/I improvement obtained, when applying a hyperstable feedback lineariser with an adaptation-law integrative gain  $k_1$  of 150 to the AM-AM and AM-PM nonlinearities of a TWTA (using the Saleh model), is greater than 28, 16, and 15 dB for 3<sup>rd</sup>-, 5<sup>th</sup>-, and 7<sup>th</sup>-order IMPs, respectively, over a 2–6-dB OBO range (with regard to P1 dB). Figure 7 shows the amelioration of impairments of this nonlinearity in eye and constellation diagrams, when applying a signal with 32 QAM and 0.35 roll-off, for low ( $k_1 = 10$ ) and high ( $k_1 = 150$ ) feedback gains, as well as versus the situation with no linearisation. In comparison with Cartesian feedback and with feedforward, the robust-

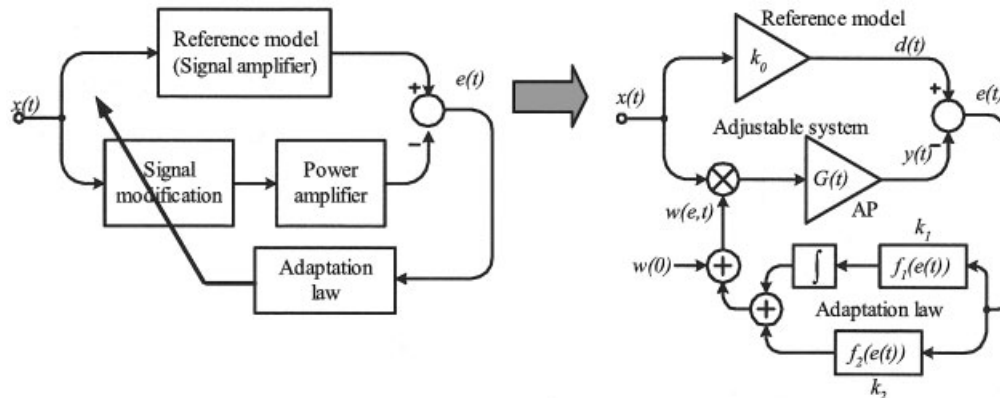
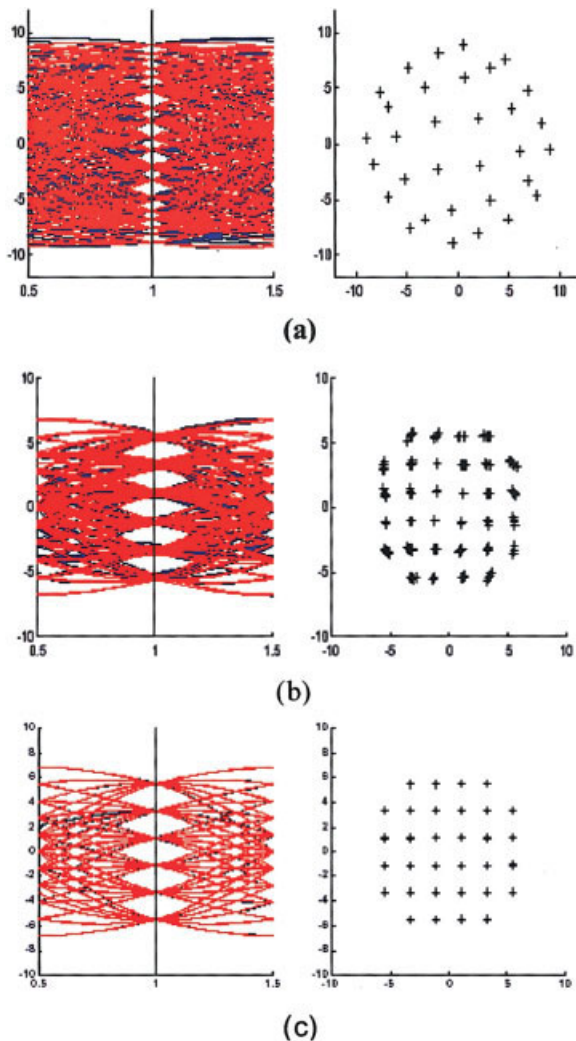


Figure 6. Hyperstable parallel model-reference adaptive system (MRAS) feedback linearisation.



**Figure 7.** Hyperstable feedback-lineariser improvements: 32-QAM, 0.35 roll-off, signal eye and constellation diagram at TWTA output with (a) no linearisation, (b)  $k_1 = 10$ , and (c)  $k_1 = 150$ . [Color figure can be viewed in the online issue, which is available at [www.interscience.wiley.com](http://www.interscience.wiley.com).]

ness of this hyperstable lineariser feedback structure is good.

Other feedback linearisation issues being considered include dynamic power supply (directed more towards power efficiency than linearisation), active bias, and thermal compensation.

## B. Feedforward

Feedforward linearisers (for example, [19–25]), among others, have reduced mathematical complexity in the control-law design, and are unconditionally stable. At least this is the case initially and before adaptivity is added. The two-path core feedforward-linearisation concept is well known. As these linearis-

ers have potential fast-response time, they are receiving much attention for linearisation solutions in broadband applications (for example, multicarrier modulations). Theoretically, this attribute is valid, but there are limitations caused by the high sensitivity to lineariser maladjustments due to their open-loop structure, component-count, and impact on PAE. For instance, incorrect physical lengths of a transmission line in each path of the feedforward structure, which directly affect the phase-shift constant of the transmission line, can reduce the operating bandwidth to a single-tone lineariser [20]. This fact is especially important when considering applications in low-wavelength carriers [25], where the electrical lengths occurring in the circuitry become comparable with the time wavelength characteristics of the signal.

The efficiency of feedforward linearisers depends on three main factors: loop imbalances, device losses, and the kind of auxiliary power amplifier used. The latter can operate at reduced backoff (relative to the main amplifier) because its input, which is theoretically composed by distortion terms, exhibits a low PAPR. Stability is an inherent property of feedforward structures. However, with a non-ideal subtract unit or finite-directivity couplers (allowing a small portion of the signal to propagate in the reverse direction, that is, feedback), the system may manifest instabilities [22]. This tendency is greater in high-gain systems and systems using broadband.

In order to achieve good signal or IMD suppression, the signals in the primary amplifying and in the distortion-cancellation paths must be balanced correctly with respect to amplitude, delay, and anti-phase. These key aspects for correct feedforward design are addressed primarily by using appropriate devices and parameter selection, mainly power combiners, subtract units, and delay compensators, where possible. Secondly, they may be addressed through adaptivity: combinations of feedforward with feedback or predistorters, as well as the use of multiple feedforward loops in a hierarchical structure, are typical system-level adaptivity solutions to help mitigate feedforward weaknesses with respect to loop maladjustments or amplifiers tolerances.

The technique of digital adaptive compensation—such as LMS and gradientlike-based methods, and correlative algorithm—aims to supervise system behaviour and, if required, take corrective actions. Hence, performance quality can be maintained throughout the system life-time. Besides development of the theoretical support, issues include the effects of imbalances and imperfect cancellation, stability, loop controllers, and the optimising algorithm, for example [19]. Analog implementations of adaptive loop con-

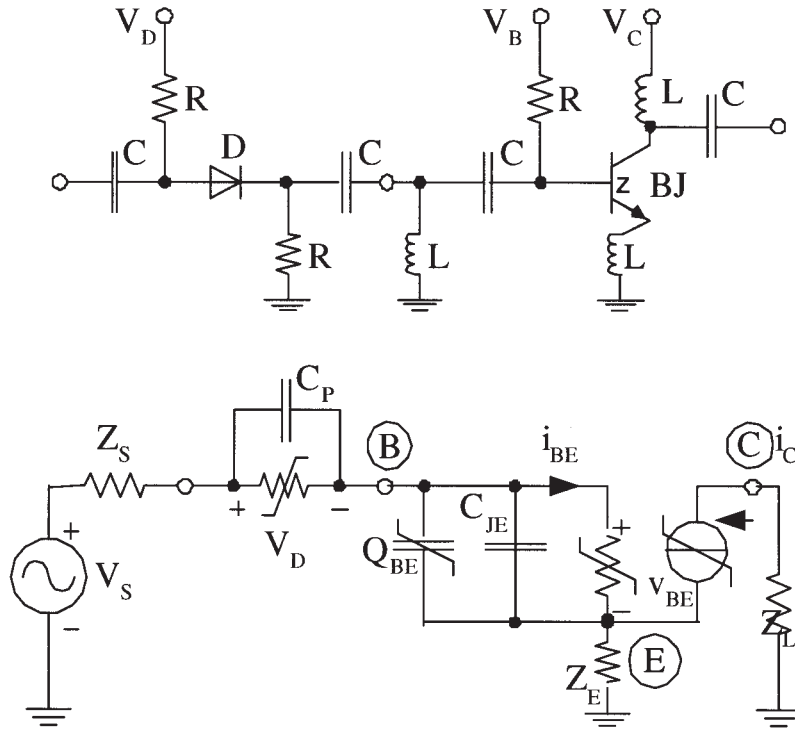


**Figure 8.** L-Band bipolar junction transistor (BJT) amplifier and series diode predistorter: simplified (a) schematic and (b) model.

trollers have been also proposed [24], which are normally based on analog versions of the LMS algorithm. Reported IMD reductions (two-tone tests) in feedforward amplifiers vary from 70 to 40 dBc in PCN basestations, and ACPR reductions over 30 dBc have been obtained in EDGE interface modulation signals.

### C. Predistortion

Predistortion techniques (see, for example, [13, 26–31]) are viewed as being of great importance because of their likely wideband application [29]. The success of predistortion relies on the accuracy of the PA characterization and the generation of an equivalent cancelling characteristic. To date, the general approach has been to assume quasi-static and memoryless approximations for the PA characteristics. Generally, the interaction between the nonlinearities present in both the predistorter and amplifier, and the noticeable memory effects, make the design and optimisation of the predistorter an involved and critical task. Techniques include RF, IF, baseband digital (in both signal- and data-predistortion approaches) and analogue predistortion. What is now perceived as being of key importance is finding techniques which will achieve real-time inverse-adaptable dynamical modelling of the PA, and this with memory effects

accounted for. Which of the existing models—Volterra, Wiener, Chebyshev, Bessel, Taylor, Saleh, and so forth—may be modified or extended in order to achieve this is an open question. New models are of course also being sought.

**A Circuit-Based RF Predistortion Scheme.** For wideband systems, RF circuit-based predistorters based on diode or transistor devices [13, 26, 14] seem to be attractive candidates. Focusing on  $\text{IMD}_3$  in a combined predistorter-PA, three main mechanisms contribute to the final result: envelope, 2<sup>nd</sup> harmonic, and third degree [27]. The pure third-degree contribution is the obvious way to generate  $\text{IMD}_3$  by a given odd-degree nonlinearity. The envelope mechanism refers to the mixing of two fundamental frequencies in a given even-degree nonlinear element followed by a new mixing with a fundamental in an even-degree nonlinearity. The 2<sup>nd</sup>-harmonic mechanism involves the generation of the 2<sup>nd</sup> harmonic of a fundamental frequency in an even-degree nonlinearity and a new even-degree mixing with another—different—fundamental. Most of the nonlinearities present in the devices contain even-degree components and, as a consequence of the envelope and 2<sup>nd</sup>-harmonic mechanisms, the linearisation performance depends

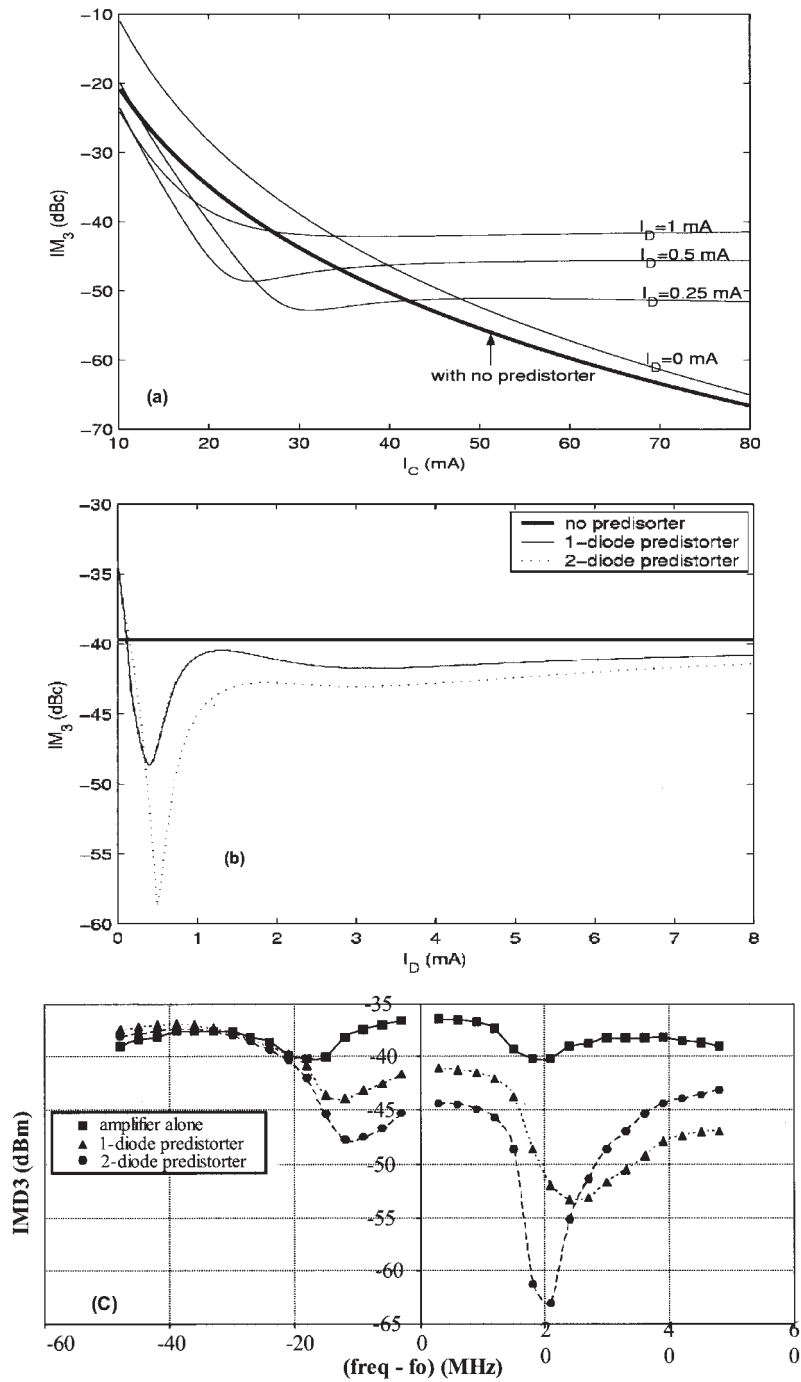


**Figure 9.** IM<sub>3</sub> results for BJT PA alone and with one- and two-diode predistorter circuits: IM<sub>3</sub> (ratio dBc and absolute dBm) and as a function of (a) the BJT collector bias current  $I_C$  for different diode bias currents  $I_D$ ; (b)  $I_D$ , and (c) offset frequency, with fixed bias for the PA and predistorter circuits.

not only on the in-band behaviour of both the amplifier and the predistorter, but also on the out-of-band impedances, thermal and trap effects, and so forth [27].

An example of a circuit-level predistortion linearisers based on diode nonlinear components

(transistors may also be used), is shown in the simplified schematic in Figure 8, together with a model of a bipolar common-emitter stage with a series predistortion diode [27]. A Volterra series analysis was carried out, which considered the contributions of all nonlinearities in the amplifier stage

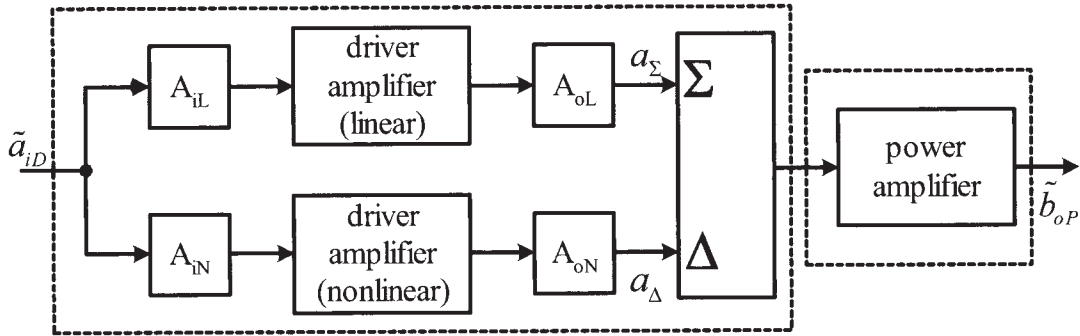


Figure 10. A predistortion scheme for a high-linearity K-band MMIC PA.

and the main nonlinearity in the diode predistorter. Currents associated with the base-charging capacitance and the collector current have been shown to be the most significant contributions to  $IM_3$ . In so far as these two currents directly depend on base-emitter diode nonlinearity, the linearisation of the transistor's base-emitter diode characteristic provides a lower  $IM_3$ . A closed-form expression for  $IM_3$  arising from the composite diode predistorter and amplifier was obtained [27]. Noting that adding two  $i$ - $v$  exponential characteristics in series, results in a softened overall  $i$ - $v$  transfer function intuitively explains how the series diode lineariser connected at the base of the bipolar stage serves to linearise the overall base diode, thus reducing the signal distortion at the amplifier output. Naturally, this “softening” will have a dependence on other conditions such as biasing.

If adding one diode to the base of the transistor smoothes the nonlinearity at the amplifier input, thus reducing the distortion at the amplifier output, one can think about adding more diodes in order to achieve a higher degree of linearisation. The series combination of two identical diodes can be thought of as one diode with a lower  $\alpha$  parameter in the diode current-source model ( $i_D = I_S[\exp(\alpha v) - 1]$ ); that is, when performing the Volterra analysis. Indeed, the results in Figure 9 show this benefit for one-diode and two-diode predistortion circuits.

It is worth noting that, even if diode predistorters can potentially offer broadband predistortion, memory in both the predistorter and amplifier circuits results in different linearisation in-band performances. As a consequence, different linearisation results can be obtained as a function of  $\Delta f$ , the two-tone spacing. The design goal should be to obtain good linearity performance over a given frequency band.

An advantage of the Volterra analysis approach is to gain insight and understanding about the interaction between nonlinearities in both the predistorter and the

amplifier. Different contributions to  $IM_3$  can be identified, isolated and this can help to optimise the design. On the other hand, it (Volterra analysis) is limited to low-order nonlinear effects and results are not accurate to high power levels.

An L-band bipolar PA, using two different diode-based predistorter circuits, has been analysed and implemented in hybrid technology using standard SMD components [27]. Analysis results of  $IM_3$  as a function of diode  $I_d$  and BJT collector bias current  $I_c$ , for a given offset frequency and compared to  $IM_3$  with no predistorter present, are shown in Figures 9(a) and 9(b); the  $IM_3$  minima may be observed. The measurement results as a function of offset frequency for the amplifier alone and the one- and two-diode predistorter circuits are also provided in Figure 9(c).

There are optimum transistor and “diode” bias points for minimum distortion. Power consumption and/or gain requirements may force a choice of a certain transistor bias point. The  $IM_3$  distortion can be optimised by varying the current through the predistortion diode. It may be noted that, in this particular circuit (diode predistorter–BJT amplifier), higher gain is achieved by increasing the diode bias current. The measurement results in Figure 9(c) show  $IMD_3$  benefits (nearly 10-dB improvement over a 20-MHz frequency bandwidth). Deep nulls appearing in the 20-MHz offset can be also observed. By adjusting the transistor bias network, it would be possible to obtain the benefit of a broader band or better results over a narrower band. The measurements show that  $IMD_5$  was in all cases well below the  $IMD_3$  products.

## B. System-Level RF Analog Predistortion

An interesting novel K-band MMIC PA predistorter [28] is illustrated by a block diagram in Figure 10. The predistortion stage has a two-branch structure. Each branch includes a driver amplifier and two

attenuators. These two driver amplifiers (DAs) and the PA are identical, except that both DAs have lower gate periphery, that is, they are scaled-down versions of the PA. Given the underlying assumption in [28] that the devices follow perfect current-scaling according to the gate periphery, this also means that the nonlinear behavior of both the DAs and the PA are identical and will have the same nonlinear describing function  $F$  as in eqs. (2) and (3) below, but the DA saturates at a lower input power. This identity makes this predistortion solution intuitively attractive. Of course, some differences may arise in practice, of which some (for example, gain) may be accounted for with modified rules for the attenuators. In the upper branch, the DA, which is driven at low input power through the high-valued attenuator ( $A_{iL}$ ), operates linearly. In the lower branch, the DA is driven into nonlinear operation through the low-valued attenuator ( $A_{iN}$ ). Through the sum and difference ports of the 180° hybrid, power from the linear and nonlinear branches is combined to create an expansive predistorter  $P_{in}$ - $P_{out}$  behavior that compensates the final PA stage compression.

Design rules for the attenuators may readily be found, assuming a simple, quasi-memoryless, narrow-band-describing function model as follows. The PA input and output envelope power waves  $\tilde{a}_{iP}$ ,  $\tilde{b}_{oP}$  are related as follows:

$$\tilde{b}_{oP} = G_p \tilde{a}_{iP} + F(|\tilde{a}_{iP}|) \tilde{a}_{iP}, \quad (2)$$

where, for both the PA and the DA,  $G_p$  is the linear gain and the (even) function  $F$  describes the nonlinear behaviour of the amplifier with input and output matching networks ( $F$  can be extracted from the large-signal  $S_{21}$  measurements).

The predistortion-stage output is the difference of the waves  $a_\Sigma$  and  $a_\Delta$  at the sum and difference port of the hybrid, respectively, and may be written as

$$a_\Sigma = G_p A_{iL} \tilde{a}_{iD} \text{ and } a_\Delta = A_{oN} G_p \tilde{a}_{iD} + A_{oN} F\left(\frac{|\tilde{a}_{iD}|}{\sqrt{k_{DP}}}\right) \tilde{a}_{iD} \quad (3)$$

where  $k_{DP}$  is a scaling factor, given as  $k_{DP} = W_D/W_P < 1$ , with  $W_D$  and  $W_P$  denoting the gate periphery count of the DA and the PA, respectively, and where the attenuators  $A_{oL}$  and  $A_{iN}$ , being redundant here, are set to one.

On substituting the “ $(a_\Sigma - a_\Delta)/\sqrt{2}$ ” difference wave into (2) and with considering only the first order

terms of a series expansion of the PA’s  $F$  (with the DA’s  $F$  function as an argument), i.e.,

$$\tilde{b}_{oP} \approx \tilde{a}_{iD} \left[ \frac{G_p^2}{\sqrt{2}} (A_{iL} - A_{oN}) - \frac{G_p A_{oN}}{\sqrt{2}} F\left(\frac{\tilde{a}_{iD}}{\sqrt{k_{DP}}}\right) + \frac{G_p}{\sqrt{2}} (A_{iL} - A_{oN}) F\left(\frac{G_p}{\sqrt{2}} \left| (A_{iL} - A_{oN}) \tilde{a}_{iD} \right| \right) \right] \quad (4)$$

the optimum values for the attenuators which yield complete cancellation of the nonlinearities, independently of the particular form of  $F$  and the power level, may be found:

$$A_{iL} = 2A_{oN}; \quad A_{oN} = \frac{\sqrt{2}}{\sqrt{k_{DP}} G_p}, \quad (5)$$

and the total transducer gain is:

$$|G_T| = \frac{|G_p|}{\sqrt{2k_{DP}}}. \quad (6)$$

With these attenuator-design rules, it can be easily verified that the nonlinear driver amplifier and the final stage are operated with the same input power and therefore produce, as expected, exactly the same nonlinearities.

The power consumption of the predistortion stage is reduced for the small-periphery devices used, and thus it has low impact on PAE, but a detailed analysis shows that the scaling factor cannot be chosen to be arbitrarily small and depends on the amplifier-power gain. It can also be demonstrated that the scheme achieves significant cancellation of the 3<sup>rd</sup>-order IMP distortion, and also partial elimination, following the same design rules, of the 5<sup>th</sup>-order IMP distortion. The former may be seen in Figure 11 for a PHEMT K-band MMIC amplifier, in class-A operation with the large-signal scattering matrix variable  $S_{21}$  obtained from an accurate finite-memory model (FMM, obtained from University of Bologna, c.f. [28]) fitted to measured data.

CAD simulations implementing the predistortion schemes show that phase-delay imbalances in the two DAs can be compensated by introducing a phase shifter in one branch of the lineariser. Small values (max. 5°) of phase shifts can significantly compensate the DA imbalance. Imperfect scaling of the DAs and the PA can lead to a different gain in the two devices; a slight modification in the optimum design rules can be made to account for this.

To achieve good IMD<sub>3</sub> performance over a broad frequency band, optimisation of the predistorter cir-

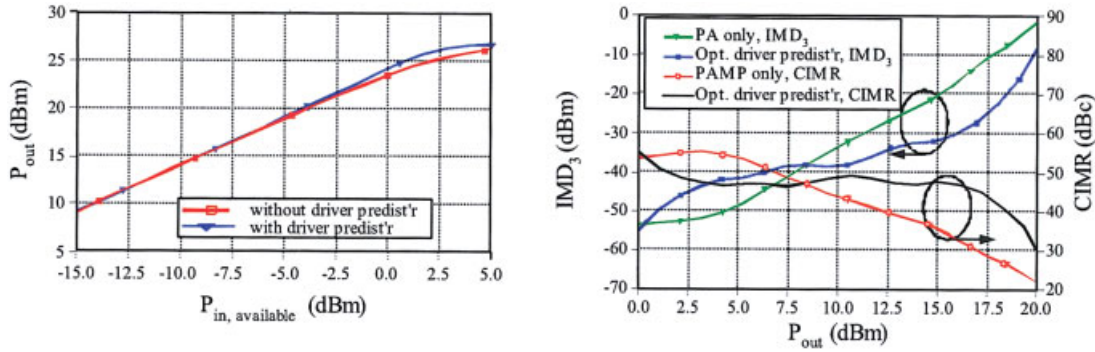


**Figure 11.** Predistortion-linearisation characteristics for a pHEMT K-band MMIC PA (class A). [Color figure can be viewed in the online issue, which is available at [www.interscience.wiley.com](http://www.interscience.wiley.com).]

cuit and low-frequency impedances in both the predistorter and the PA is required. In addition to the complex nonlinear phenomena, short- and long-term memory effects are issues to be considered carefully in this optimisation process.

### C. System-Level Digital Predistortion

In digital signal predistortion, the coefficients of the predistorter polynomial, which are related to the PA distortion curves, are allocated in a look-up table (LUT). The coefficients are precomputed for the non-adaptive approach and are continuously adjusted in the adaptive case. Active research on the reduction of the computational effort and LUT memory requirement is ongoing.

Also at the system level, data predistortion is attracting attention as a solution that shows good in-band linearization performance. Its operation is quite intuitive: from data-constellation measurements from the PA, the predistorter modifies, in both magnitude and phase, the points of the input data constellation. A drawback of the method to date is its lack of control on the ACI. However, it does yet again draw attention to the question of what empirical information may usefully and robustly be fed back in order to enable good lineariser adaptability.

**Other Techniques.** Other techniques, which some researchers might categorise among the types already mentioned, include EER, LINC, and combined analogue-locked loop universal modulator (CALLUM), which is a modification of the LINC structure that provides Cartesian feedback to compensate gain- and phase-imbalance problems. LINC and CALLUM require a DSP because they require the computation of an inverse cosine term. EER using switching-mode power supplies is one of the techniques currently being considered for DVB-T, and important research

is focused on reducing the time constants that limit applicability in high-speed applications. Finally, pseudo-linearisation techniques, for example, power combiners and Doherty amplifiers [32], are also available.

### V. ADAPTIVITY

To obtain the most benefit from the lineariser, it should be matched to the particular amplifier. However, the amplifier characteristics will vary either intentionally (for example, with bias point under a transmit power control protocol) or unintentionally (for example, tolerances in their fabrication or self-heating effects). With respect to the latter, the temperature sensitivity of the SSPA RF performance is a key linearisation-adaptivity issue, as mentioned above in reference to Figure 1.

Robust adaptability of the linearisation characteristics to match PA variations, and the capturing of suitable control signals for this adaptation, is an important area of research. Some forms of adaptivity, especially feedback, are discussed above. Linearisers that do not adapt or adapt poorly can of course add to the nonlinearity problem rather than ameliorate it. Here, the challenging issues of direct or indirect measurement of device dynamic characteristics, especially of memory and thermal effects, together with their multilevel model design are present, for example [7]. This kind of research work is still in its early stages.

### VI. CONCLUSION

TARGET sees linearisation techniques at the circuit and system levels as a key research issue today for modern evolving advanced wireless transmitters from

embedded mobile and handheld terminals, to base stations, HAPs, and satellites. A key driver is the competing requirements of improved signal fidelity and PA-system PAE, over a range of contexts from single and multicarrier NoCEM air-interface modes to simultaneous multimode-transmitter systems. At present, solutions offer finite though modest linearity improvements, which are a function of the air-interface mode. Their adequacy depends on the context, but they can help achieve linearity goals in tandem with other options. Nevertheless, different practical and challenging problems—many of which have yet to be fully understood and characterised, such as memory effects, self-heating effects, interaction between nonlinearities, and stability issues—may reduce potential performance.

## ACKNOWLEDGMENTS

This work was based upon work supported by TARGET—“Top Amplifier Research Groups in a European Team”—an EU Network of Excellence, FP6-IST-2004-507893 (see [www.target-net.org](http://www.target-net.org))

## REFERENCES

1. G. Magerl, M. Mayer, F. Giannini, M.S. O'Droma, A. Mediavilla, A. Cidronali, W. Richter, J. P. Teyssier, P. Colantonio, D. Schreurs, R. Makri, T.J. Brazil, and G. Manes, et al., Top amplifier research group in a European team (TARGET): NoE Description of Work. Annex I, Project proposal, 2004.
2. J.J. Brown, J.A. Pusch, M. Hu, A.E. Schmitz, D.P. Docter, J.B. Shealy, M.G. Case, and M.A. Thompson, High-efficiency GaAs-based pHEMT C-band power amplifier, *IEEE Microwave Wireless Compon Lett* 6 (1996), 91–93.
3. S.L.G. Chu, A. Platzker, M. Borkowski, R. Mallavarpu, M. Snow, A. Bowlby, D. Teeter, T. Kazior, and K. Alavi, A 7.4 to 8.4 GHz high-efficiency PHEMT three-stage power amplifier, *IEEE MTT-S Int Microwave Symp Dig* 2 (2000), 947–950.
4. J.B. Johnson, A.J. Joseph, D.C. Sheridan, R.M. Maladi, P.O. Brandt, J. Person, J. Andersson, A. Bjorneklett, U. Pearson, F. Abasi, and L. Tilly, Silicon-germanium BiCMOS HBT technology for wireless power amplifier applications, *IEEE Int J Solid-State Electron* 39 (2004), 1605–1614.
5. V. Paidi, S. Xie, R. Coffie, B. Moran, S. Heikman, S. Keller, A. Chini, S.P. DenBaars, U.K. Mishra, S. Long, and M.J.W. Rodwell, High-linearity and high-efficiency of class-B power amplifiers in GaN HEMT technology, *IEEE Trans Microwave Theory Tech* 51 (2003), 643–652.
6. Y.H. Wang, H.Z. Liu, H.K. Huang, and C.C. Wang, L-band, high-efficiency 25-Watt power amplifier using PHEMT for Base station system, *IEEE Electron Devices Microwave and Optoelectronic Applic* (2003), 76–82.
7. W. Bosch and G. Gatti, Measurement and simulation of memory effects in predistortion linearizers, *IEEE Trans Microwave Theory Tech* 37 (1989), 1885–1890.
8. F. Cappelluti, F. Bonani, S. Donati Guerrieri, G. Ghione, C.U. Naldi, M. Peroni, A. Cetronio, and R. Graffitti, Self-consistent fully dynamic electro-thermal simulation of power HBTs, GAAS'01. London, U.K., 2001., pp. 199–202.
9. M.S. O'Droma and N. Mgebrishvili, Signal modelling classes for linearised OFDM SSPA behavioural analysis, *IEEE Commun Lett* 9 (2005), 127–129.
10. J.C. Pedro and N.B. Carvalho, *Intermodulation distortion in microwave and wireless circuits*, Artech House, Boston, 2003.
11. M. O'Droma and N. Mgebrishvili, On quantifying the benefits of SSPA linearisation in UWC-136 systems, *IEEE Trans Signal Processing* 53 (2005), 2470–2476.
12. M. O'Droma, N. Mgebrishvili, and A. Goacher, New percentage linearization measures of the degree of linearization of HPA nonlinearity, *IEEE Commun Lett* 8 (2004), 214–216.
13. S. Cripps, *Advanced techniques in RF power amplifier design*, Artech House, Boston, 2002.
14. F.H. Raab, P. Asbeck, S. Cripps, P.B. Kenington, Z.B. Popovic, N. Potheary, J.F. Sevic, and N.O. Sokal, Power amplifiers and transmitters for RF and microwave, *IEEE Trans Microwave Theory Tech* 50 (2002), 814–826.
15. A. Anakabe, J.-M. Collantes, J. Portilla, J. Jugo, A. Mallet, L. Lapierre, and J.-P. Frayssé, Analysis and elimination of parametric oscillations in monolithic power amplifiers, *IEEE MTT-S IMS* 3 (2002), 2181–2184.
16. D. Gil and J. Jugo, Eliminación de distorsión en amplificadores de RF mediante realimentación pasiva, *URSI, Spanish Chapter, A Coruña*, 2003.
17. E. Bertran, Montoro, G., Model reference linearization based on H-infinity control, S. Kozak (Ed.), *New Trends in Design of Control Systems; IFAC, Smolenice: Pergamon Press, New York*, 1997, pp. 77–82.
18. A.J. Zozaya and E. Bertran, Passivity theory applied to the design of power amplifier linearizers, *IEEE Trans Vehic Technol* 50 (2004), 1126–1137.
19. M.E. Gadringer, H. Arthaber, and G. Magerl, Loop controller for a feedforward amplifier minimizing the measured power signal, *Proc RAWCON '03, Boston, MA*, 2003, 281–284.
20. S.-G. Kang, I.-K. Lee, and K.-S. Yoo, Analysis and design of feedforward power amplifier, *IEEE MTT-S IMS* 3 (1997), 1519–1522.
21. P. Kenington, High-linearity RF amplifier design, Artech House, Boston, 2000.
22. P.B. Kenington, P.A. Warr, and R.J. Wilkinson, Analysis of instability in feedforward loop, *Electron Lett* 33 (1997), 1669–1671.

23. N. Pothecary, Feedforward linear power amplifiers, Artech House, Boston, 1999.
24. A. Zozaya, E. Bertran, and J. Berenguer-Sau, Adaptive feedforward amplifier linearizer using analog circuitry, *Microwave J* 44 (2001), 102–114.
25. A.J. Zozaya and E. Bertran, On the performance of Cartesian feedback and feedforward linearization structures operating at 28 GHz, *IEEE Trans Broadcasting* 50 (2004), 382–389.
26. J. Kim and K. Konstantinou, Digital predistortion of wideband signals based on power amplifier model with memory, *Electron Lett* 37 (2001), 1417–1418.
27. L. León and J. Portilla, Predistorsión a diodo en amplificadores bipolares bajo régimen débilmente o lineal, *URSI, Spanish Chapter, A Coruña*, 2003.
28. P. Bianco, S. Donati Guerrieri, G. Ghione, M. Pirola, C.U. Naldi, C. Florian, G. Vannini, A. Santarelli, F. Filicori, L. Manfredi, Optimum design of a new pre-distortion scheme for high linearity K-band MMIC power amplifiers, *GAAS'01, London, UK*, 2001, pp. 689–692.
29. J. Vuolevi, J. Manninen, and T. Rahkonen, Cancelling the memory effects in RF power amplifiers, *IEEE Int Symp Circ Syst* 1 (2001), 57–60.
30. J. Yi, Y. Yang, M. Park, W. Kang, and B. Kim, Analog predistortion linearizer for high-power RF amplifiers, *IEEE Trans MTT* 48 (2000), 2709–2713.
31. A. Zhu and T.J. Brazil, An adaptive Volterra predistorter for the linearization of RF high power amplifiers, *IEEE MTT-S Int Microwave Symp Dig* 1 (2002), 461–464.
32. J.R. Gajadharsing, O. Bosma, and P. van Westen, Analysis and design of a 200-W LDMOS-based Doherty amplifier for 3-G base stations, *IMS, Fort Worth, TX*, 2004, pp. 529–532.

## BIOGRAPHIES



**Máirtín S. O'Droma** B.E., Ph.D., C.Eng., F.IEE, IEEE (S.M.), received his bachelor's and doctoral degrees from the National University of Ireland in 1973 and 1978, respectively. He is a Senior Lecturer and Director of the Telecommunications Research Centre, University of Limerick, Ireland. His current activities include serving as founding partner and steering committee member, TARGET—"Top Amplifier Research Groups in a European Team"—the EU FP6 Network of Excellence IST-507893 (2004–2008), and section head of the RF power linearisation and amplifier-modeling research strand; founding partner and steering committee member, AN-WIRE—Academic Network for Wireless Internet Research in Europe—the EU FP5 Thematic Network of Excellence IST-38835 (2002–2004); Member of two European "Cooperation in the field of Science and Technology Research Actions" (COST Actions 285 and 290). His previous posts include Lecturer at the National University of Ireland, Dublin and at the National University of Ireland, Galway, Director of Communications Software Ltd., and ODR Patents Ltd. His research interests include complex telecommunication-systems simulation and behavioural modeling, linearisation and efficiency techniques in multimode, multicarrier ultra-broadband nonlinear microwave and mm-wave transmit-power amplifiers; smart adaptive antenna arrays and MIMO channels; and network and protocol infrastructural innovations for evolving new wireless-telecommunication paradigms.



**Eduard Bertran** received his Ingeniero (option in communication electronics) and Doctor Ingeniero degrees in telecommunication engineering, both from the Universitat Politècnica de Catalunya (UPC), Barcelona, Spain, in 1979 and 1985, respectively. He joined the department of Signal Theory and Communications (TSC), Universitat Politècnica de Catalunya, in 1987, where he is currently a Full Professor. He has been the Head of Studies of the TSC Department and an Associate Dean in different telecommunication schools. His research interests include control, communication electronics, signal processing, and circuit theory, topics about which he has produced different books and peer-reviewed journal and conference papers. He is a member of IFAC and a senior member of IEEE (secretary of the Spanish Section). He has collaborated in different national and European research projects and teams.



**Joaquín Portilla** was born in St. Gilles-Croix de Vie, France, on May 23, 1967. He received his degree in electronic physics from the University of Cantabria, Spain, in 1990 and his Ph.D. degree in electrical engineering from IRCOM, University of Limoges, France, in 1994. From 1994 to 1997, he was with the Communications Engineering Department of the University of Cantabria, Spain, involved in the design of hybrid and monolithic microwave circuits for communication systems. In 1997 and 1998 he worked for IFCA (Physics Institute of Cantabria), Spain, where he was involved in the analysis and design of low-noise circuits and receivers for microwave remote sensing. In 1998, he joined the Electricity and Electronics Department of the University of the Basque Country as an Associate Professor, where he is engaged in the analysis and design of RF and microwave circuits and systems.



**Nana Mgebrishvili**, B.S., Ph.D., MIEE, MIEEE, received her bachelor's degree in telecommunications engineering from Georgian Technical University, Georgia, in 2000 and her Ph.D. degree from the University of Limerick, Ireland, in 2004. She participates as a researcher in the TARGET—"Top Amplifier Research Groups in a European

Programme Network of Excellence, EU FP6 NoE IST-507893 and in the ANWIRE—"Academic Network for Wireless Internet Research in Europe," a European Union FP5 Thematic Network of Excellence IST-38835. Her research interests include modeling and simulation, linearisation and efficiency techniques of ultra-broadband nonlinear high-power amplifiers. She is presently Quality Assurance Manager, MagtiCom Ltd., Georgia.



**Simona Donati Guerrieri** was born in 1969 in Milano, Italy. She received her degree in theoretical physics in 1993 from the University of Milano and her Ph.D. in electron devices from University of Trento in 1999. She is presently working as a Researcher in the Electronics Department of the Politecnico di Torino, where she joined the microwave electronics group. Her research interests

include the modeling and simulation of microwave solid-state devices, including physics-based noise analysis, and the RF and microwave integrated-circuit design. She has been an IEEE member since 1997.



**Gabriel Montoro López** was born in Barcelona, Spain. He received his degree in Telecommunication Engineering from the Universitat Politècnica de Catalunya (UPC) in 1989 and did his final project at the area of Adaptive Control. He joined the department of Signal Theory and Communications (TSC) in 1991, where he is currently an Associate Professor. He received his Ph.D.

degree in telecommunications in 1996, with "robust control" the central core of his Ph.D. thesis. He is a Lecturer on pregraduate courses at the Escola Politècnica Superior de Castelldefels (EPSC). He also teaches postgraduate courses on Adaptive and Non-Linear Systems. His research interests include control and consumer and communications electronics.



**Thomas J. Brazil**, B.E., Ph.D., FIEI, FIEEE, MRSA, received his B.E. degree in electrical engineering from University College Dublin in 1973, and was awarded his Ph.D. degree in electronic engineering by the National University of Ireland in 1977. He subsequently worked on microwave subsystem development at Plessey Research (Caswell) U.K., before returning to UCD in 1980. He

now holds the Chair of Electronic Engineering at UCD and is also Head of the Department of Electronic and Electrical Engineering. His research interests are in the fields of nonlinear modelling and characterisation techniques at the device, circuit, and system levels. He also has interests in nonlinear simulation algorithms and several areas of microwave subsystem design and applications. He has published widely in the international scientific literature in these fields. He has been actively involved in EU Framework Programme research for almost 20 years, including acting as project coordinator, evaluator, and reviewer of major projects and acting as policy advisor to the European Commission. He is Head of the Microwave Research Group at UCD, while also acting as the Associate Dean for Research in the Faculty of Engineering, and he is one of six elected Professors on the University's Governing Authority. He is a member of IEEE MTT-1 Technical Committee on Computer-Aided Design, and from 1998–2001, was appointed by the IEEE Microwave Theory and Techniques Society as a Worldwide Distinguished Lecturer in High-Frequency CAD Applied to Wireless Systems. He is a Fellow of the Institution of Engineers of Ireland and was elected a Fellow of the IEEE in 2003. He was recently elected a Member of the Royal Irish Academy. He will be Chair of the European Microwave Conference in the U.K. in 2006.



**Gottfried Magerl** was born in Vienna, Austria. He received both his Dipl.-Ing. and the Dr. techn. degrees from the Vienna University of Technology in 1972 and 1975, respectively. Since 1973 he has been with the Institute of Communications and Radio Frequency Engineering. In 1981 he was appointed Academic Lecturer (Universitätsdozent), and in 1990 he became University

Professor of Microwave Engineering. In 1998 he became Head of the Institute of Electronic Design and Measurement Techniques at the Vienna University of Technology. He spent the academic year 1981–82 and the summer months of 1984 and 1986 at the University of Chicago and at the University of Michigan, East Lansing, where he constructed high-resolution IR spectrometers based on the microwave modulation of CO<sub>2</sub> and CO lasers via the electrooptic effect in CdTe. In the following, his interests in the application of electromagnetic radiation to noncontacting measurement techniques lead to the development of a road-condition-sensing microwave radar and to extensive work on physics and optimization of narrowband atomic line filters. At present, his research interests concentrate on the development of highly-efficient linear microwave power amplifiers for mobile communications. Since 2004, he is Scientific Co-ordinator of the EC FP6 network of excellence TARGET—"Top Amplifier Research Groups in a European Team."